Computers and Concrete, *Vol. 16, No. 2 (2015) 223-243*
DOI: http://dx.doi.org/10.12989/cac.2015.16.2.223

Instantaneous and time-dependent flexural cracking models of reinforced self-compacting concrete slabs with and without fibres

Farhad Aslani[*1], Shami Nejadi[2] and Bijan Samali[3]

[1]*Centre for Infrastructure Engineering and Safety, School of Civil and Environmental Engineering, University of New South Wales, Australia*
[2]*School of Civil and Environmental Engineering, University of Technology Sydney, Australia*
[3]*Institute for Infrastructure Engineering, University of Western Sydney, Australia*

(Received December 1, 2014, Revised July 1, 2015, Accepted July 10, 2015)

Abstract. Self-compacting concrete (SCC) can be placed and compacted under its own weight with little or no compaction. It is cohesive enough to be handled without segregation or bleeding. Modifications in the mix design of SCC may significantly influence the material's mechanical properties. Therefore, it is vital to investigate whether all the assumed hypotheses about conventional concrete (CC) are also valid for SCC structures. The aim in this paper is to develop analytical models for flexural cracking that describe in appropriate detail the observed cracking behaviour of the reinforced concrete flexural one way slabs tested. The crack width and crack spacing calculation procedures outlined in five international codes, namely Eurocode 2 (1991), CEB-FIP (1990), ACI318-99 (1999), Eurocode 2 (2004), and fib-Model Code (2010), are presented and crack widths and crack spacing are accordingly calculated. Then, the results are compared with the proposed analytical models and the measured experimental values, and discussed in detail.

Keywords: self-compacting concrete; crack width; crack spacing; flexural cracking; time-dependent cracking; analytical models

1. Introduction

When a reinforced concrete member is subjected to a bending moment, two types of stresses (longitudinal and lateral stresses) act on the tensile zones of the concrete surrounding the tensile reinforcement (as shown in Fig. 1). The tensile zone undergoes a lateral contraction before cracking when the longitudinal bending stress acts. Also, it is resulting in lateral compression between the reinforcing bar and the concrete around it. When a flexural crack starts to develop, this biaxial lateral compression has to disappear at the crack because the longitudinal tension in the concrete becomes zero. The stress in the concrete is dynamically transferred to the reinforcing bar and the tensile stress in the concrete becomes zero at the cracked section. The position of the

[*] Corresponding author, Ph.D., E-mail: F.Aslani@unsw.edu.au

http://www.techno-press.org/?journal=cac&subpage=8 ISSN: 1598-8198 (Print), 1598-818X (Online)

neutral axis rises at the cracked section in order to maintain equilibrium at that section (Mari *et al.* 2010, Gribniak *et al.* 2013, Aslani 2014).

Tensile stress is present in the concrete between the cracks, because tension is transferred from the steel to the concrete by bond. The distribution of tensile stress in the concrete and the steel depends on the magnitude and distribution of bond stress between the cracks. Longitudinal bond stress exists between the concrete and the tensile reinforcement in the regions adjacent to each crack and this gradually builds up the stress in the concrete on either side of the crack. Further loading causes the tensile stress to increase until the tensile strength of the concrete at the next weakest section of the reinforced concrete member is exceeded and this section also cracks. With increasing load, this process continues until the distance between the cracks is not large enough for the extreme fibre tensile stress to reach the tensile strength of the concrete and hence to cause cracking. Once this stage is reached, the crack pattern has stabilized and further loading just widens the existing cracks. The distance between two adjacent cracks at this stage is called the stabilized crack spacing. The width of each of the two cracks in Fig. 1 is essentially a function of the difference in elongation between the reinforcing bars and the surrounding concrete in tension over a length distance between two adjacent cracks (Bischoff 2003, Nejadi 2005, Chiaia *et al.* 2008, Gilbert and Ranzi 2011, Vasanelli *et al.* 2013).

Self-compacting concrete (SCC) can be placed and compacted under its own weight with little or no vibration and without segregation or bleeding. SCC is used to facilitate and ensure proper filling and good structural performance of restricted areas and heavily reinforced structural members. It has gained significant importance in recent years because of its advantages. Recently, this concrete has gained wider use in many countries for different applications and structural configurations. SCC can also provide a better working environment by eliminating the vibration noise. Such concrete requires a high slump that can be achieved by superplasticizer addition to a concrete mix and special attention to the mix proportions. SCC often contains a large quantity of powder materials that are required to maintain sufficient yield value and viscosity of the fresh mix, thus reducing bleeding, segregation, and settlement. As the use of a large quantity of cement increases costs and results in higher temperatures, the use of mineral admixtures such as fly ash, blast furnace slag, or limestone filler could increase the slump of the concrete mix without increasing its cost (Aslani and Nejadi 2012 a, b, Aslani 2013, 2015).

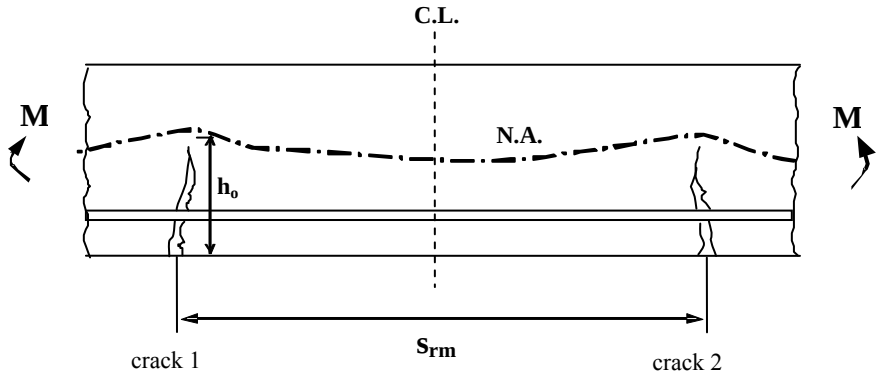

Fig. 1 Illustrative sustained loads slab specimens

Moreover, fibre-reinforced self-compacting concrete (FRSCC) is a relatively recent composite material that combines the benefits of the SCC technology with the advantages of the fibre addition to a brittle cementitious matrix. It is a ductile material that in its fresh state flows into the interior of the formwork, filling it in a natural manner, passing through the obstacles, and flowing and consolidating under the action of its own weight. FRSCC can mitigate two opposing weaknesses: poor workability in fibre-reinforced concrete (FRC) and cracking resistance in plain concrete (Mazzotti and Savoia 2009, Aslani and Nejadi 2012 c, d, e).

To control the crack width at the flexural member tension surface, designers can use the guidelines prescribed in various design codes. These guidelines are based on certain analytical solutions to crack width for conventional concrete (CC) that were developed by various researchers. There is no study about analytical models for instantaneous and time-dependent flexural cracking of reinforced SCC and FRSCC one way slabs.

2. Research significance

In this study, the experimental results of eight flexural one way slabs under sustained service loads for periods up to 240 days are used for proposing analytical models for instantaneous and time-dependent flexural cracking of reinforced SCC and FRSCC members. Four SCC mixes-two plain SCC (N-SCC), two steel fibre (D-SCC), two polypropylene fibre (S-SCC), and two hybrid fibre (DS-SCC) FRSCC one way slabs-are considered in the analysis (Aslani *et al.* 2014 a, b). Crack width, crack patterns, deflections at mid-span, steel strains and concrete surface strains at the steel levels were recorded at each load increment in the post-cracking range and all these results are used for verifying the proposed models. This is the first research that has been done on the analytical instantaneous and time-dependent flexural cracking of reinforced SCC and FRSCC in the world.

3. SCC and FRSCC slabs specimens

A total of eight SCC and FRSCC slabs with the same cross-section and details were monitored for up to 240 days to measure the time-dependent development of cracking and deformations under service loads. A general view of the test specimens is shown in Fig. 1. The slab specimens were each nominally 3500 mm long by 400 mm wide. In all slabs the nominal distance from the soffit to the centroid of the main reinforcement was 25 mm. Slabs series were each reinforced with 4N12. The parameter is varied in the tests, including the four SCC mixes-one control SCC mixture (N-SCC) and three fibre-reinforced SCC mixtures were used in this study. Fibre-reinforced SCC mixtures contain steel (D-SCC), PP (S-SCC), and hybrid (steel + PP) (DS-SCC) fibres (Aslani and Nejadi 2013 a, b). All slab specimens were subjected to different gravity loads, consisting of self-weight plus superimposed sustained loads via carefully constructed and arranged concrete blocks supported off the top (of the specimens). To provide the sustained loading, rectangular concrete blocks of predetermined size and weights were cast and weighed prior to the commencement of the test. The blocks were suitably arranged on the top surface of each specimen to achieve the desired sustained load level. Two sustained load levels were considered, namely 50% and 30% of the ultimate design load, and designated load conditions ‘a’ and ‘b’, respectively. The slab specimens were subjected to uniformly distributed sustained loads, UDL + self-weight.

All measurements were taken within the high moment region, i.e. the middle third of the span for beams and for slabs where M ≥ 90% Mmax (Aslani 2014).

4. Crack width and crack spacing according to the codes of practice

In this section, the crack width and crack spacing calculation procedures outlined in five international concrete codes, namely Eurocode 2 (1991), CEB-FIP (1990), ACI318-99 (1999), Eurocode 2 (2004), and fib-Model Code (2010), are presented. Results are compared with the analytical model proposed here and with the measured experimental values. Crack width is not specifically mentioned as a design parameter in AS 3600. AS 3600 (2009) is adopted the Eurocode 2 recommendations. In AS 3600 (2009), Section 4, "Crack control of slabs" is described as follow:

Cracking in reinforced slabs subject to flexure shall be deemed to be controlled if the appropriate requirements in below items are satisfied. For areas of slabs fully enclosed within a building except for a brief period of weather exposure during construction and, where it is assessed that crack control is not required, only Item (a) and Item (b) need be satisfied.

a) The minimum area of reinforcement in a tensile zone of a slab supported by columns at their corners complies with [0.24 $(D/d)^2 f'_{ct.f}/f_{sy}$] or of a slab supported by beams or walls on four sides complies with [0.19 $(D/d)^2 f'_{ct.f}/f_{sy}$].

b) The centre-to-centre spacing of bars in each direction shall not exceed the lesser of 2.0 D_s or 300 mm. Bars with a diameter less than half the diameter of the largest bar in the cross-section shall be ignored.

c) The calculated tensile steel stress shall not exceed the larger of the maximum steel stresses.

d) The calculated tensile steel stress shall not exceed 0.8 f_{sy}.

5. Flexural cracking model for CC by Nejadi (2005)

In the Nejadi's (2005) proposed model, Tension Chord Model, T.C.M (Marti *et al.* 1998) has been incorporated into the idealized model to represent the tensile zone of the cracked member. Obviously, as the applied moment M increases, the tension stiffening effect decreases and the contribution of the tensile concrete between the cracks to the stiffness of the member decreases. This phenomenon can be modelled by reducing the effective tensile area of the concrete, A_{cti} or by reducing the average concrete tensile stress, σ_{cti} as moment increases. In the present section, A_{cti} is assumed to be constant after cracking and independent of the applied moment and time. However, σ_{cti} is assumed to depend on the applied moment and reduces with time due to creep and shrinkage.

From the Nejadi's (2005) experimental and numerical study, the effective tensile area of concrete, A_{cti} surrounding the flexural tensile reinforcement and having the same centroid as that of reinforcement may be expressed as follows

For slabs

$$A_{cti} = 2\, n_b\, d_c\, R_f\, s \tag{1}$$

$$R_f = 0.31\,(n_b - 1) \le 1 \tag{2}$$

where D is the depth of section, b is the width of section, d_n is the depth of compression zone in a fully cracked section, dc is the distance from the centre of reinforcement bar to extreme tensile

fibre, s is the bar spacing, n_b is the number of reinforcing bar ($n_b \geq 2$).

According to the T.C.M. (Marti *et al.* 1998), the concrete in the tension chord is assumed to carry a uniform average tensile stress, σ_{cti}. The instantaneous average tensile stress, σ_{cti} under short-term service loads can be determined from below Eq. as follow

$$\sigma_{cti} = \frac{\tau_{bi}\ s_{rm}\ \rho_{ef}}{d_b} \tag{3}$$

where τ_{bi} is the short-term bond stress, ρ_{ef} is the effective reinforcement ratio (ratio of tensile reinforcement area to the area of the effective concrete in tension, A_{st}/A_{cti}), A_{st} is the cross-sectional area of tensile steel reinforcement, A_{cti} is the intact area of tensile concrete; s_{rm} is the average crack spacing, and d_b is the nominal diameter of the tensile reinforcing bars.

The force in the bar is transmitted to the surrounding concrete by bond shear stress, τ_b. Due to this force transfer, the force in a reinforcing bar changes along its length. The bond shear stress depends on several factors, including the concrete tensile strength and cover, steel stress, bar size and spacing, confining effects, and load history. From the Nejadi (2005) experimental results presented, bond shear stress τ_b decreases with increasing steel stress and reduces under sustained load with time. Marti *et al.* (1998) is assumed $\tau_{bi} = \tau_{bo} = 2\ f_{ct}$ for the service load range ($\sigma_s < f_{sy}$) and f_{ct} is the direct tensile strength of concrete.

$$\tau_b = \lambda_1\ \lambda_2\ \lambda_3\ f_{ct} \tag{4}$$

where λ_1 accounts for the load duration with λ_1 =1.0 for short-term calculations and λ_1 = 0.7 for long-term calculations, λ_2 is a factor that accounts for the reduction in bond stress as the steel stress σ_{st1} (in MPa) increases

$$\lambda_2 = 1.66 - 0.003\ \sigma_{st1} \geq 0.0 \tag{5}$$

and λ_3 is a factor that accounts for the very significant increase in bond stress that has been observed in laboratory tests for small diameter bars (Gilbert and Nejadi 2004) and may be taken as

$$\lambda_3 = 7.0 - 0.3\ d_b \geq 2.0 \tag{6}$$

Also, Nejadi (2005) proposed instantaneous crack width model as

$$(w_i)_{tc} = \frac{s}{E_s}\left[\frac{T}{A_{st}} - \frac{\tau_b\ s}{d_b}\left(1 + n\rho_{tc}\right)\right] \tag{7}$$

Moreover, the proposed time-dependent crack width model by Nejadi (2005) is as below Eq.

$$(w^*)_{soffit} = \frac{s^*}{E_s}\left[\frac{T}{A_{st}} - \frac{\tau_b\ s^*}{d_b}\left(1 + n_e\ \rho_{tc}\right) - \varepsilon_{sh}\ E_s\right] \tag{8}$$

6. Proposed flexural cracking models for SCC and FRSCC

The proposed models in this study for prediction of instantaneous and time-dependent crack widths for SCC and FRSCC are based on the proposed models by Leutbecher (2007) that are summarized through Sections 6.1-6.4. The Leutbecher and Fehling's (2008) proposed models are

including instantaneous and time-dependent crack widths for initial crack and stabilized cracking phases. These models are proposed for conventional reinforced concrete (CRC) and CRC with fibres. The flexural cracking modelling of fibre reinforced concrete is very complicated but the proposed model by Leutbecher (2007) are very convenient and effective for both instantaneous and time-dependent cracking modelling of this type of concrete. The proposed models of Leutbecher (2007) are more suitable when they are combined with the proposed effective tensile area of concrete Eq. (1) by Nejadi (2005) and the calculated results are more in agreement with the measured experimental results. Also, in accordance with the experimental study presented in Aslani *et al.* (2014 a, b), the proposed bond shear stress for short-term and long-term behaviour which have been applied in the crack width and spacing calculations based on the Leutbecher (2007)'s models can be presented as follows

For short-term

N-SCC: $$\tau_b = \begin{cases} 1.50\ f_{ct} & \sigma_{s,max} < 180\ MPa \\ 1.50\ f_{ct} & f_{sy} > \sigma_{s,max} \geq 180\ MPa \end{cases} \quad (9)$$

D-SCC: $$\tau_b = \begin{cases} 1.25\ f_{ct} & \sigma_{s,max} < 180\ MPa \\ 1.30\ f_{ct} & f_{sy} > \sigma_{s,max} \geq 180\ MPa \end{cases} \quad (10)$$

S-SCC: $$\tau_b = \begin{cases} 1.50\ f_{ct} & \sigma_{s,max} < 180\ MPa \\ 1.70\ f_{ct} & f_{sy} > \sigma_{s,max} \geq 180\ MPa \end{cases} \quad (11)$$

DS-SCC: $$\tau_b = \begin{cases} 1.50\ f_{ct} & \sigma_{s,max} < 180\ MPa \\ 1.60\ f_{ct} & f_{sy} > \sigma_{s,max} \geq 180\ MPa \end{cases} \quad (12)$$

All the N-SCC, D-SCC, S-SCC, DS-SCC mixtures for the long-term behaviour

$$\tau_b = 1.5\ f_{ct} \quad (13)$$

The proposed models for calculation of instantaneous and time-dependent crack widths for SCC and FRSCC are presented in Section 6.5.

6.1 Calculation of instantaneous and time-dependent crack widths in conventional reinforced concrete-initial cracking

Leutbecher (2007) have derived a cracking model based on the assumptions of constant bond stress and a parabolic development of concrete and steel strains between the cracks. To calculate crack widths, the assumption of parabolic strain development is used to determine mean steel and concrete strains. The maximum crack width is calculated as twice the transfer length multiplied by the difference between the concrete and steel mean strains. The calculation of the instantaneous crack widths of RC member (as shown in Fig. 2) follows below the steps

$$F = F_c + F_s = \sigma_c\ A_c + \sigma_s\ A_s \Rightarrow \varepsilon_c = \varepsilon_s \Rightarrow \sigma_c = E_c\ \varepsilon_c^I \text{ and } \sigma_s = E_s\ \varepsilon_s^I: \quad (14)$$

$$\sigma_c = \frac{F}{A_c\left(1 + \alpha_E\ \rho_s\right)} \quad (15)$$

$$F_{cr} = A_c \left(1 + \alpha_E \ \rho_s\right) f_{ct} \tag{16}$$

$$\sigma_s = \left(1 + \alpha_E \ \rho_s\right) \frac{f_{ct}}{\rho_s} \tag{17}$$

$$l_{es} = \frac{\sigma_s \ d_b}{4 \ \tau_{sm} \left(1 + \alpha_E \ \rho_s\right)} = \frac{f_{ct} \ d_b}{4 \ \tau_{sm} \ \rho_s} \tag{18}$$

$$w = 2 \, l_{es} \left(\varepsilon_{sm} - \varepsilon_{cm}\right) \tag{19}$$

$$\varepsilon_{sm} = \left(1 - \alpha_b\right) \varepsilon_s^{II} + \alpha_b \ \varepsilon_s^{I} \tag{20}$$

$$\varepsilon_{cm} = \alpha_b \ \varepsilon_c^{I} = \alpha_b \ \varepsilon_s^{I} \tag{21}$$

$$w = \frac{\left(1 - \alpha_b\right) \sigma_s^2 \ d_b}{2 \ E_s \ \tau_{sm} \left(1 + \alpha_E \ \rho_s\right)} = \frac{\left(1 - \alpha_b\right) f_{ct}^2 \ d_b}{2 \ E_s \ \tau_{sm} \ \rho_s^2} \left(1 + \alpha_E \ \rho_s\right) \tag{22}$$

where w_{max} is the maximum crack width, l_{es} is the transfer length, ε_{sm} is the mean steel strain, ε_{cm} is the mean concrete strain, F_{cr} is the cracking force, σ_s is the steel stress, τ_{sm} is the average bond stress over the load transmission length, f_{ct} is the concrete matrix tensile strength, d_s is the reinforcing bar diameter, E_s is the modulus of elasticity of reinforcing bar, ρ_s is the reinforcing ratio of steel reinforcement; α_b is the shape coefficient of the strains (α_b = 0.6 for short term loading, α_b = 0.4 for long term or repeated loading), α_E is the ratio of the modulus of elasticity of steel to the modulus of elasticity of concrete ($\alpha_E = E_s/E_c$). Fig. 2 shows definitions of the various strains that are used in this model.

The calculation of crack widths of RC member with initial crack by considering the influence of shrinkage and creep (as shown in Fig. 3) can be presented as follows

shrinkage strain without creep effect: $$\varepsilon_{s.shr} = \frac{\varepsilon_{cs}}{1 + \alpha_E \ \rho_s} \tag{23}$$

shrinkage strain with creep effect: $$\varepsilon_{s.shr} = \frac{\varepsilon_{cs}}{1 + \alpha_E \ \rho_s \left(1 + \rho \varphi\right)} \tag{24}$$

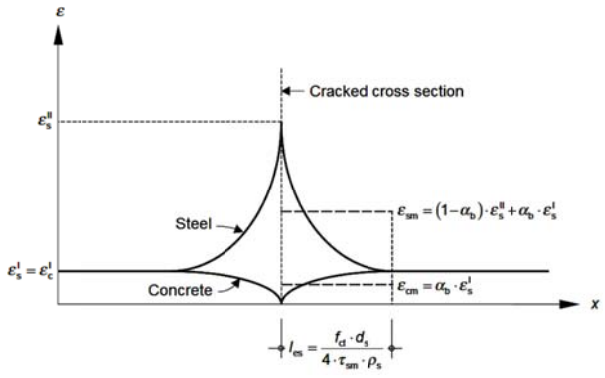

Fig. 2 Initial crack - Qualitative distribution of strains for the steel bar and the matrix (Leutbecher 2007)

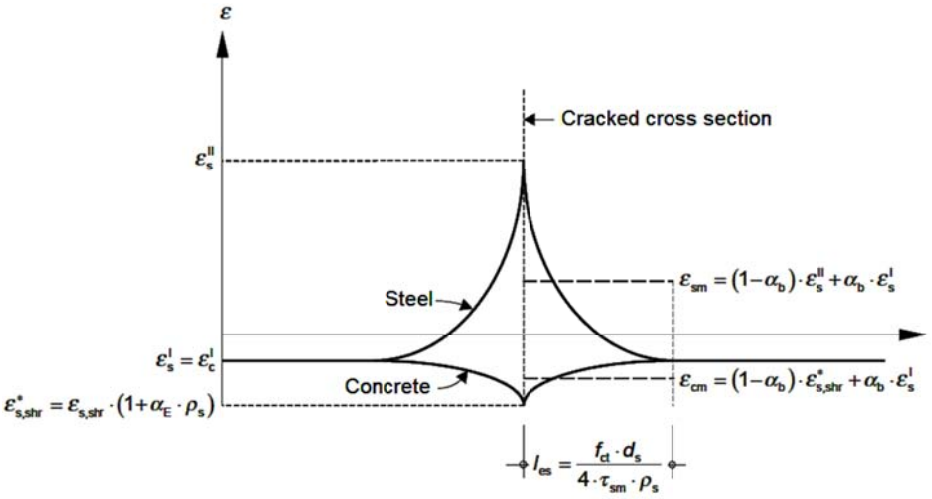

Fig. 3 Initial crack-qualitative distribution of strains for the steel bar and the matrix, considering the influence of shrinkage (Leutbecher 2007)

where ρ is the relaxation coefficient equal to 0.8 and φ is the creep coefficient.

$$F_{cr} = A_c \left(1 + \alpha_E \, \rho_s\right)\left(f_{ct} + \varepsilon_{s,shr} \, E_s \, \rho_s\right) \tag{25}$$

$$\sigma_s = \left(1 + \alpha_E \, \rho_s\right)\left(\frac{f_{ct}}{\rho_s} + \varepsilon_{s,shr} \, E_s\right) \tag{26}$$

$$\varepsilon_{s.shr}^{*} = \varepsilon_{s.shr}\left(1 + \alpha_E \, \rho_s\right) \tag{27}$$

$$l_{es} = \frac{\left(\dfrac{\sigma_s}{1 + \alpha_E \, \rho_s} - \varepsilon_{s,shr} \, E_s\right) d_b}{4 \, \tau_{sm}} = \frac{f_{ct} \, d_b}{4 \, \tau_{sm} \, \rho_s} \tag{28}$$

$$\varepsilon_{sm} = \left(1 - \alpha_b\right) \varepsilon_s^{II} + \alpha_b \, \varepsilon_s^{I} \tag{29}$$

$$\varepsilon_{cm} = \left(1 - \alpha_b\right) \varepsilon_{s,shr}^{*} + \alpha_b \, \varepsilon_c^{I} = \left(1 - \alpha_b\right) \varepsilon_{s,shr}^{*} + \alpha_b \, \varepsilon_s^{I} \tag{30}$$

$$w = 2\frac{\left(\dfrac{\sigma_s}{1 + \alpha_E \, \rho_s} - \varepsilon_{s,shr} \, E_s\right) d_b}{4 \, \tau_{sm}}\left[\left(1 - \alpha_b\right)\varepsilon_s^{II} - \left(1 - \alpha_b\right)\varepsilon_{s,shr}^{*}\right] \tag{31}$$

$$w = \frac{\left(1 - \alpha_b\right)\left(\dfrac{\sigma_s}{1 + \alpha_E \, \rho_s} - \varepsilon_{s,shr} \, E_s\right)^2 d_b}{2 \, E_s \, \tau_{sm}}\left[1 + \alpha_E \, \rho_s\right] \tag{32}$$

Fig. 3 shows definitions of the various strains that are used in this model.

6.2 Calculation of instantaneous and time-dependent crack widths in conventional reinforced concrete - stabilized cracking

Similarly, Leutbecher (2007) cracking model is applicable to the stabilizing cracking too. Calculation of crack widths of CRC member with stabilized cracking (as shown in Fig. 4) can be shown as follows

For $s_r = s_{r,max} = 2\, l_{es}$

$$\varepsilon_{sm} = \varepsilon_s^{II} - \alpha_b \frac{f_{ct}}{\rho_s\, E_s} \tag{33}$$

$$\varepsilon_{cm} = \alpha_b \frac{f_{ct}}{E_c} = \alpha_b \frac{f_{ct}}{\rho_s\, E_s}\, \alpha_E\, \rho_s \tag{34}$$

$$w_{max} = s_{r,max}\left(\varepsilon_{sm} - \varepsilon_{cm}\right) = \frac{f_{ct}\, d_b}{2\, E_s\, \tau_{sm}\, \rho_s}\left[\sigma_s - \alpha_b \frac{f_{ct}}{\rho_s}\left(1 + \alpha_E\, \rho_s\right)\right] \tag{35}$$

For $s_{r,min} = l_{es} \le s_r < s_{r,max} = 2\, l_{es}$

$$\varepsilon_{sm} = \varepsilon_s^{II} - \alpha_b \frac{2\, s_r\, \tau_{sm}}{d_b\, E_s} \tag{36}$$

$$\varepsilon_{cm} = \alpha_b \frac{2\, s_r\, \tau_{sm}\, \rho_s}{d_b\, E_s} = \alpha_b \frac{2\, s_r\, \tau_{sm}}{d_s\, E_s}\, \alpha_E\, \rho_s \tag{37}$$

$$w = s_r\left(\varepsilon_{sm} - \varepsilon_{cm}\right) = \frac{s_r}{E_s}\left[\sigma_s - \alpha_b \frac{2\, s_r\, \tau_{sm}}{d_b}\left(1 + \alpha_E\, \rho_s\right)\right] \tag{38}$$

Calculation of the crack widths for CRC member with stabilized cracking by considering the influence of shrinkage (as shown in Fig. 5) follows the below steps

For $s_r = s_{r,max} = 2\, l_{es}$

$$\varepsilon_{sm} = \varepsilon_s^{II} - \alpha_b \frac{f_{ct}}{\rho_s\, E_s} \tag{39}$$

$$\varepsilon_{cm} = \alpha_b \frac{f_{ct}}{\rho_s\, E_s} \alpha_E\, \rho_S + \varepsilon_{s,shr}^{*} \tag{40}$$

$$w_{max} = s_{r,max}\left(\varepsilon_{sm} - \varepsilon_{cm}\right) = \frac{f_{ct}\, d_b}{2\, E_s\, \tau_{sm}\, \rho_s}\left[\sigma_s - \left(\alpha_b \frac{f_{ct}}{\rho_s} + \varepsilon_{s,shr}\, E_s\right)\left(1 + \alpha_E \rho_s\right)\right] \tag{41}$$

For $s_{r,min} = l_{es} \le s_r < s_{r,max} = 2\, l_{es}$

$$\varepsilon_{sm} = \varepsilon_s^{II} - \alpha_b \frac{2 s_r\, \tau_{sm}}{d_b\, E_s} \tag{42}$$

$$\varepsilon_{cm} = \alpha_b \frac{s_r}{d_b} \frac{2\,\tau_{sm}}{E_s} \alpha_E \rho_S + \varepsilon^*_{s,shr} \tag{43}$$

$$w = s_r \left(\varepsilon_{sm} - \varepsilon_{cm}\right) = \frac{s_r}{E_s}\left[\sigma_s - \left(\alpha_b \frac{2\,s_r\,\tau_{sm}}{d_b} + \varepsilon_{s,shr}\,E_s\right)\left(1+\alpha_E\,\rho_s\right)\right] \tag{44}$$

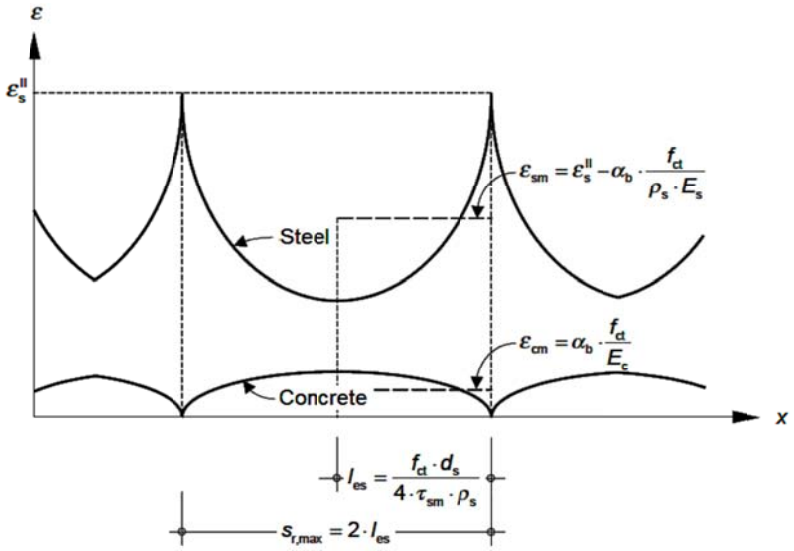

Fig. 4 Stabilized cracking - Qualitative distribution of strains for the steel bar and the matrix (Leutbecher 2007)

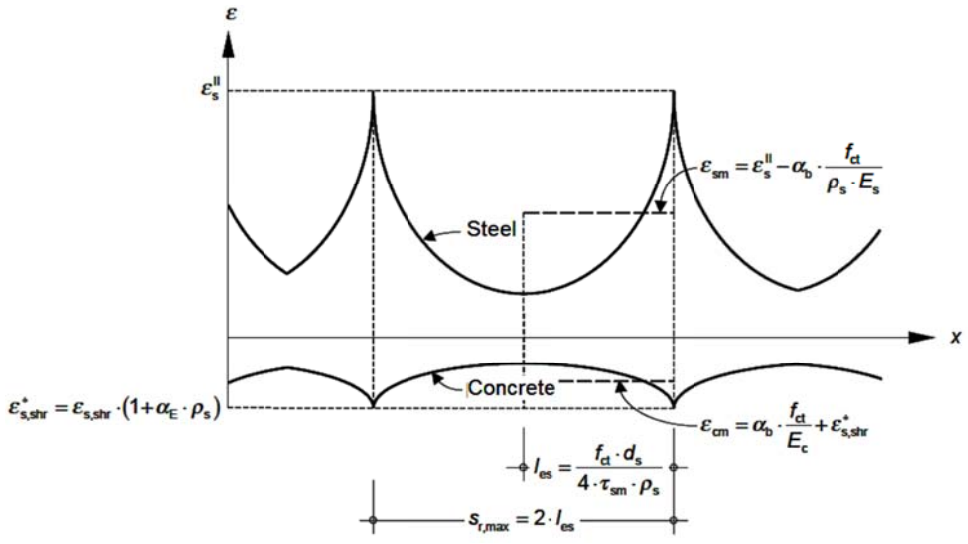

Fig. 5 Stabilized cracking - Qualitative distribution of strains for the steel bar and the matrix, considering the influence of shrinkage (Leutbecher 2007)

6.3 Calculation of instantaneous and time-dependent crack widths in conventional reinforced concrete with fibres - initial cracking

Calculation of the instantaneous crack widths of CRC with fibres member with initial crack (as shown in Fig. 6) can be presented as follows

$$F_{cr} = A_c \left(1 + \alpha_{E,s}\ \rho_s / \gamma\right)\left(\sigma^i_{cf,cr} + \varepsilon_{s,shr}\ E_s\ \rho_s\right) \tag{45}$$

$$\sigma^i_{c,cr} = \left(1 + \alpha_{E,s}\ \rho_s / \gamma\right)\left(\sigma^i_{cf,cr} + \varepsilon_{s,shr}\ E_s\ \rho_s\right) \tag{46}$$

$$\sigma^i_{cf,cr} = \frac{E_f^2\ d_f}{16\ \tau_f\ l_f}\left(1 - \sqrt{1 + \frac{16\ \tau_f}{E_f\ d_f}\left(w - \frac{l_f}{2}\right)}\right)^2 \tag{47}$$

$$\alpha_{E,s} = \frac{E_s}{E_c} \tag{48}$$

$$\rho_s = \frac{A_s}{A_c} \tag{49}$$

$$\gamma = 1 + \rho_f\ \left(\eta\ \alpha_{E,f} - 1\right) \tag{50}$$

where ρ_f is the fibre content and η is the fibre orientation coefficient.

$$w_s = 2\ l_{es}\ \left(\varepsilon_{sm} - \varepsilon_{cm}\right) = \frac{\left(1 - \alpha_b\right)\left[\sigma_s - \dfrac{\sigma^i_{cf,cr}\ \alpha_{E,s}}{\gamma}\right] d_b}{2\ E_s\ \tau_{sm}}\left(\sigma_s\right) \tag{51}$$

Calculation of the crack widths of CRC with fibres member with initial crack by considering the influence of shrinkage (as shown in Fig. 7) can be shown as follows

$$\varepsilon^*_{shr} = \varepsilon_{s,shr}\ \left(1 + \alpha_{E,s}\ \rho_s / \gamma\right) + \varepsilon_{f,shr}\ \alpha_{E,f}\ \eta\ \rho_f \tag{52}$$

where $\varepsilon_{f,shr}$ is the shrinkage shortening of the fibres.

$$\alpha_{E,f} = \frac{E_f}{E_c} \tag{53}$$

$$\varepsilon^{I-II}_s = \varepsilon^{I-II}_c = \varepsilon_{s,shr}\ \left(1 + \alpha_{E,s}\ \rho_s / \gamma\right) + \frac{\sigma^i_{cf,cr}\ \alpha_{E,s}}{\gamma\ E_s} \tag{54}$$

$$l_{es} = \frac{\left[\sigma_s - \varepsilon_{s,shr}\ E_s\ \left(1 + \alpha_{E,s}\ \rho_s / \gamma\right) - \dfrac{\sigma^i_{cf,cr}\ \alpha_{E,s}}{\gamma}\right] d_b}{4\ \tau_{sm}} \tag{55}$$

$$\varepsilon_{sm} = \left(1 - \alpha_b\right)\varepsilon^{II}_s + \alpha_b\ \varepsilon^{I-II}_s \tag{56}$$

$$\varepsilon_{cm} = (1-\alpha_b)\varepsilon_{shr}^{II} + \alpha_b\ \varepsilon_c^{I-II} \tag{57}$$

$$w_s = 2\,l_{es}\,(\varepsilon_{sm} - \varepsilon_{cm}) = \frac{(1-\alpha_b)\left[\sigma_s - \varepsilon_{s,shr}\ E_s\,(1+\alpha_{E,s}\,\rho_s/\gamma) - \dfrac{\sigma_{cf,cr}^{i}\,\alpha_{E,s}}{\gamma}\right] d_b}{2\,E_s\,\tau_{sm}}\left(\sigma_s - \varepsilon_{shr}^{*}\,E_s\right) \tag{58}$$

Fibre activation phase

$$\varepsilon_{cm} = (1-\alpha_b)\varepsilon_{shr}^{II} + \alpha_b\ \varepsilon_c^{I-II} \tag{59}$$

Fibre pullout phase

$$l_{fbs} = \frac{\sigma_f\ d_f}{8\,\tau_f} \tag{60}$$

$$\varepsilon_{f,shr}^{*} = \varepsilon_{f,shr}\ \gamma \tag{61}$$

Fibre activation phase

$$w_f = \frac{\left(\sigma_f - \varepsilon_{f,shr}^{*}\ E_f\right) d_f}{4\,E_f\ \tau_f}\left(\sigma_f + \varepsilon_{f,shr}^{*}\ E_f - 2\,\varepsilon_{shr}^{*}\ E_f\right) \tag{62}$$

Fibre pullout phase

$$w_f = \frac{l_f}{2} - \frac{\sigma_f\ d_f}{4\,\tau_f} + \frac{\left(\sigma_f - \varepsilon_{f,shr}^{*}\ E_f\right) d_f}{4\,E_f\ \tau_f}\left(\sigma_f + \varepsilon_{f,shr}^{*}\ E_f - 2\,\varepsilon_{shr}^{*}\ E_f\right) \tag{63}$$

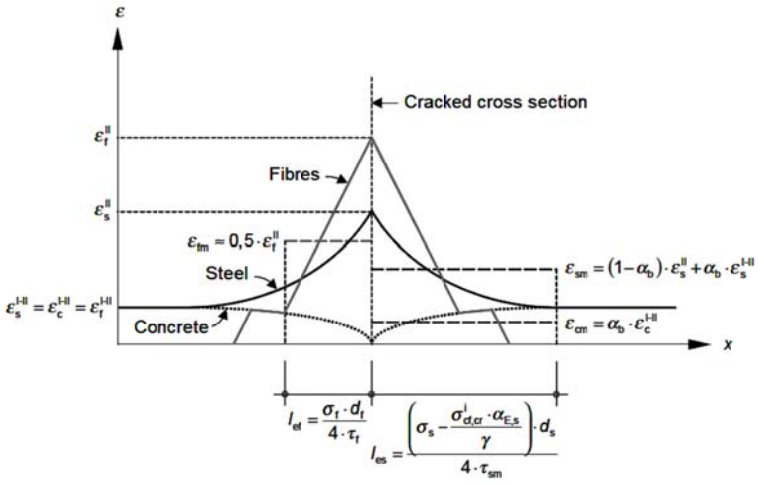

Fig. 6 Initial crack-Qualitative distribution of strains for the steel bar and fibres reinforcement and the matrix (Leutbecher 2007)

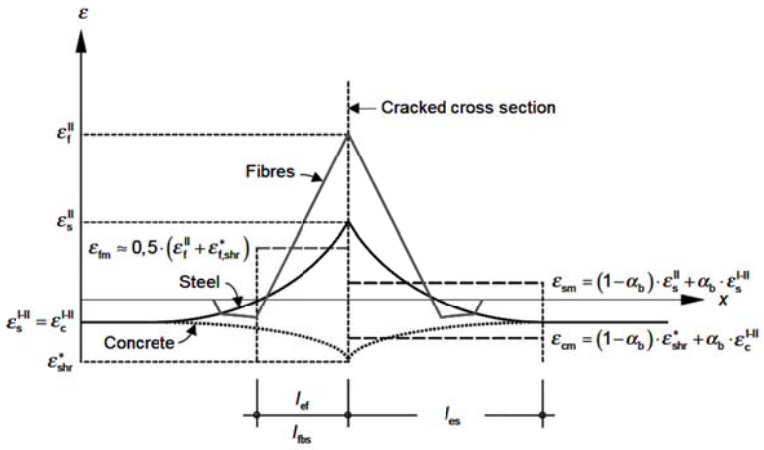

Fig. 7 Initial crack - Qualitative distribution of strains for the steel bar and fibres reinforcement and the matrix, considering the influence of shrinkage (Leutbecher 2007)

6.4 Calculation of instantaneous and time-dependent crack widths in conventional reinforced concrete with fibres - stabilized cracking

Calculation of the instantaneous crack widths of CRC with fibres member with stabilized cracking (as shown in Fig. 8) can be presented as follows

$$\varepsilon_{sm} = \varepsilon_s^{II} - \alpha_b \frac{2\, s_r\, \tau_{sm}}{d_b\, E_s} \tag{64}$$

$$\varepsilon_{cm} = \alpha_b \left(\frac{2\, s_r\, \tau_{sm}}{d_b\, E_s} \alpha_{E,s}\, \rho_s / \gamma + \frac{\sigma_{cf}}{\gamma\, E_s} \alpha_{E,s} \right) \tag{65}$$

$$w_s = s_r \left(\varepsilon_{sm} - \varepsilon_{cm} \right) = s_r \left[\frac{\sigma_s}{E_s} - \alpha_b \left(\frac{2\, s_r\, \tau_{sm}}{d_b\, E_s} \left(1 + \alpha_{E,s}\, \rho_s / \gamma \right) + \frac{\sigma_{cf}}{\gamma\, E_s} \alpha_{E,s} \right) \right] \tag{66}$$

Calculation of the crack widths of CRC with fibres member with stabilized cracking by considering the influence of shrinkage (as shown in Fig. 9) can be shown as follows

$$\varepsilon_{sm} = \varepsilon_s^{II} - \alpha_b \frac{2\, s_r\, \tau_{sm}}{d_b\, E_s} \tag{67}$$

$$\varepsilon_{cm} = \alpha_b \left(\frac{2\, s_r\, \tau_{sm}}{d_b\, E_s} \alpha_{E,s}\, \rho_s / \gamma + \frac{\sigma_{cf}}{\gamma\, E_s} \alpha_{E,s} - \varepsilon_{f,shr}^{*}\, \alpha_{E,f}\, \eta\, \rho_f \right) + \varepsilon_{shr}^{*} \tag{68}$$

$$w_s = s_r \left(\varepsilon_{sm} - \varepsilon_{cm} \right) =$$
$$s_r \left[\frac{\sigma_s}{E_s} - \alpha_b \left(\frac{2\, s_r\, \tau_{sm}}{d_b\, E_s} \left(1 + \alpha_{E,s}\, \rho_s / \gamma \right) + \frac{\sigma_{cf}}{\gamma\, E_s} \alpha_{E,s} - \varepsilon_{f,shr}^{*}\, \alpha_{E,f}\, \eta\, \rho_f \right) - \varepsilon_{shr}^{*} \right] \tag{69}$$

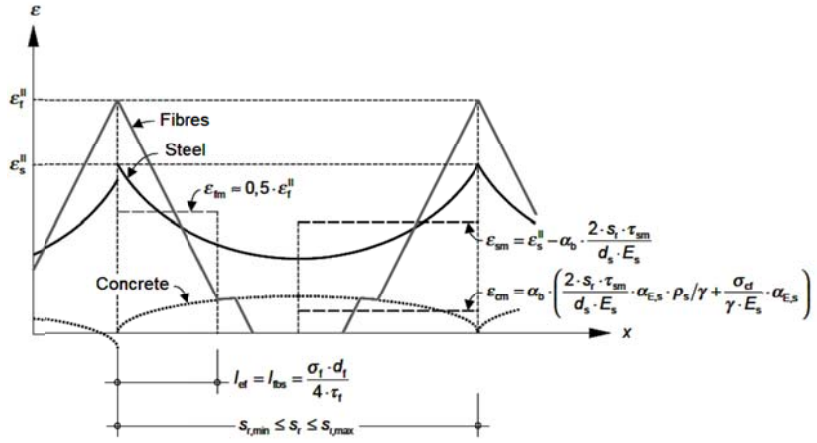

Fig. 8 Stabilized cracking-qualitative distribution of strains for the steel bar and fibres reinforcement and the matrix (Leutbecher 2007)

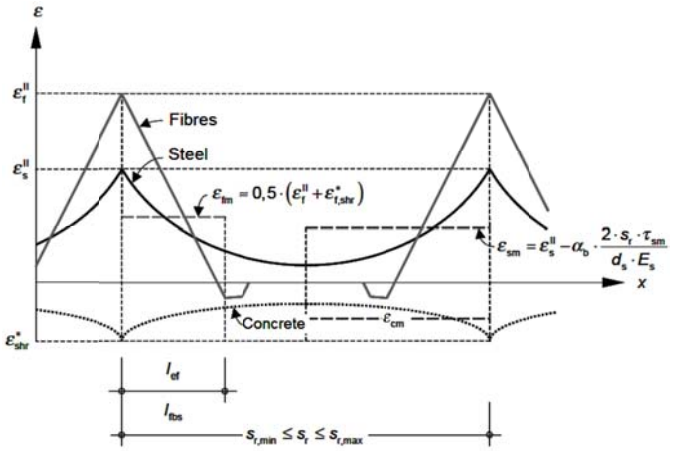

Fig. 9 Stabilized cracking-qualitative distribution of strains for the steel bar and fibres reinforcement and the matrix, considering the influence of shrinkage (Leutbecher 2007)

6.5 Proposed models for calculation of instantaneous and time-dependent crack widths and crack spacing for SCC and FRSCC

Proposed SCC and FRSCC flexural cracking models-instantaneous and time-dependent behaviour are presented through Table 1. In these equations, the proposed these bond shear stress models, Eqs. (9)-(13), should be used.

7. Discussion of the results

Rational analytical models are presented for predicting the crack width and crack spacing of flexural SCC and FRSCC slabs. The proposed analytical models were used to predict crack width

and crack spacing of eight flexural slabs under sustained service loads for periods up to 240 days. It should be emphasized that, cracking in reinforced concrete is a random phenomenon and measured crack widths and crack spacing in structural members show large scatter. Considering this, good agreement was both obtained between the measured experimental values and the predicted values.

In order to make a comparison between the models, crack width and crack spacing were also calculated in accordance with Eurocode 2 (1991), CEB-FIP (1990), ACI318-99 (1999), Eurocode 2 (2004), fib-Model Code (2010), Nejadi (2005), Leutbecher (2007), and proposed model in this study. Comparison between the experimental results, proposed analytical model and international codes are presented in Tables 2-5 and illustrated in Figs. 10 and 11.

7.1 Crack width

The instantaneous behaviour of Eurocode 2 (1991) overestimates the crack width for slab specimens at all steel stress levels. However, for long-term behaviour, it underestimates actual crack widths. The instantaneous crack widths calculated in accordance with CEB-FIP (1990) at in-service steel stress levels up to 250 MPa underestimates the crack width for slab specimens. However, for time-dependent behaviour, the method slightly underestimates the crack width at steel stress levels lower than 200 MPa and for slabs with widely spaced tensile reinforcement bars.

The instantaneous crack widths calculated in accordance with ACI318-99 (1999) at steel stress levels up to 250 MPa shows that ACI318-99 overestimates the crack width for slab specimens at all steel stress levels. Since in this code the time-dependent effect of shrinkage has not been considered, ACI318-99 (1999) underestimates the long-term crack width.

For the instantaneous behaviour, Eurocode 2 (2004) slightly underestimates the crack width for slab specimens at all steel stress levels. However, for long-term behaviour, it more underestimates actual crack widths. The instantaneous crack widths calculated in accordance with fib-Model Code (2010) at in-service steel stress levels up to 250 MPa slightly overestimates the crack width for slab specimens. However, for time-dependent behaviour, the method underestimates the crack width at steel stress levels lower than 200 MPa and for slabs with widely spaced tensile reinforcement bars.

The instantaneous crack widths calculated in accordance with Nejadi (2005) and Leutbecher (2007) at in-service steel stress levels up to 250 MPa underestimate the crack width for slab specimens. However, for time-dependent behaviour, the methods slightly underestimate the crack width at steel stress levels lower than 200 MPa and for slabs with widely spaced tensile reinforcement bars. The crack widths calculated in accordance with Proposed Model at steel stress levels up to 250 MPa shows that, for short-term cracking and time-dependent behaviour, Proposed Model predicts crack widths in good agreement with measured experimental results at all steel stress levels.

7.2 Crack spacing

Instantaneous crack spacing reduces with time under sustained load due to creep and shrinkage. Eurocode 2 (1991), CEB-FIP (1990), fib-Model Code (2010), and Leutbecher (2007) give equations corresponds to the design or characteristic maximum crack width and consider the limit values of maximum crack width under quasi-permanent loading as satisfactory for reinforced concrete members. Therefore, crack spacing calculated in accordance with the above mentioned

Table 1 Proposed SCC and FRSCC flexural cracking models

Proposed models	Equations
instantaneous crack width initial crack phase - SCC	$w = \dfrac{0.25\, f_{ct}^2\, d_b}{E_s\, \tau_b\, \rho_s^2}\left(1+\dfrac{E_s}{E_c}\rho_s\right)$
time-dependent crack width initial crack phase - SCC	$w = \dfrac{0.25\left(\dfrac{\sigma_s}{1+\dfrac{E_s}{E_c}\rho_s} - \varepsilon_{s,shr}\, E_s\right)^2 d_b}{E_s\, \tau_b}\left[1+\dfrac{E_s}{E_c}\,\rho_s\right]$
instantaneous crack width stabilized cracking phase - SCC	$w = \dfrac{s_r}{E_s}\left[\sigma_s - \dfrac{s_r\, \tau_b}{d_b}\left(1+\dfrac{E_s}{E_c}\,\rho_s\right)\right]$
time-dependent crack width stabilized cracking phase - SCC	$w = \dfrac{s_r}{E_s}\left[\sigma_s - \left(\dfrac{s_r\, \tau_b}{d_b} + \varepsilon_{s,shr}\, E_s\right)\left(1+\dfrac{E_s}{E_c}\rho_s\right)\right]$
instantaneous crack width initial crack phase - SCC	$w_s = \dfrac{0.25\left[\sigma_s - \dfrac{\sigma_{cf,cr}^i \dfrac{E_s}{E_c}}{\gamma}\right] d_b}{E_s\, \tau_b}(\sigma_s)$
instantaneous crack width initial crack phase - FRSCC	$w_s = \dfrac{0.25\left[\sigma_s - \dfrac{\sigma_{cf,cr}^i \dfrac{E_s}{E_c}}{\gamma}\right] d_b}{E_s\, \tau_b}(\sigma_s)$
time-dependent crack width initial crack phase - FRSCC	$w_s = \dfrac{0.25\left[\sigma_s - \varepsilon_{s,shr}\, E_s\left(1+\dfrac{E_s}{E_c}\rho_s/\gamma\right) - \dfrac{\sigma_{cf,cr}^i \dfrac{E_s}{E_c}}{\gamma}\right] d_b}{E_s\, \tau_b}\left(\sigma_s - \varepsilon_{shr}^*\, E_s\right)$
instantaneous crack width stabilized cracking phase - FRSCC	$w_s = s_r\left[\dfrac{\sigma_s}{E_s} - \left(\dfrac{s_r\, \tau_b}{d_b\, E_s}\left(1+\dfrac{E_s}{E_c}\,\rho_s/\gamma\right) + \dfrac{\sigma_{cf}}{\gamma\, E_c}\right)\right]$
time-dependent crack width stabilized cracking phase - FRSCC	$w_s = s_r\left[\dfrac{\sigma_s}{E_s} - \left(\dfrac{s_r\, \tau_{sm}}{d_b\, E_s}\left(1+\dfrac{E_s}{E_c}\,\rho_s/\gamma\right) + \dfrac{\sigma_{cf}}{\gamma\, E_c} - \varepsilon_{f,shr}^*\,\dfrac{E_f}{E_c}\eta\,\rho_f\right) - \varepsilon_{shr}^*\right]$
instantaneous and time-dependent crack spacing	$(s_r)_{max} = \dfrac{f_{ct}\, d_b}{2\,\tau_b\, \rho_{ef}}$; $(s_r)_{min} = \dfrac{1}{2}(s_r)_{max}$; $(s_r)_{ave} = \dfrac{(s_r)_{max} + (s_r)_{min}}{2}$

Table 2 Comparison between crack widths experimental results, proposed analytical model and codes for instantaneous behaviour

Instantaneous behaviour				
Mixes	N-SCC-a	N-SCC-b	D-SCC-a	D-SCC-b
Experimental Results	0.1100	0.0800	0.1100	0.0700
Eurocode 2 (1991)	0.1396	0.0831	0.1396	0.0831
CEB-FIP (1990)	0.0741	0.0392	0.0591	0.0566
ACI318-99 (1999)	0.1785	0.1311	0.1783	0.1310
Eurocode 2 (2004)	0.0961	0.0509	0.0767	0.0314
fib-Model Code (2010)	0.1213	0.0981	0.1093	0.0743
Nejadi (2005)	0.0857	0.0543	0.0886	0.0561
Leutbecher (2007)	0.0667	0.0319	0.0506	0.0292
Proposed Model	0.1040	0.0751	0.1057	0.0685
Mixes	S-SCC-a	S-SCC-b	DS-SCC-a	DS-SCC-b
Experimental Results	0.1200	0.0700	0.1000	0.0600
Eurocode 2 (1991)	0.1396	0.0831	0.1396	0.0831
CEB-FIP (1990)	0.0748	0.0473	0.0664	0.0399
ACI318-99 (1999)	0.1783	0.1310	0.1782	0.1309
Eurocode 2 (2004)	0.1066	0.0613	0.0969	0.0517
fib-Model Code (2010)	0.1180	0.0996	0.1173	0.0997
Nejadi (2005)	0.1003	0.0558	0.0768	0.0573
Leutbecher (2007)	0.0772	0.0424	0.0610	0.0261
Proposed Model	0.1184	0.0657	0.0933	0.0575

Table 3 Comparison between crack spacing experimental results, proposed analytical model and codes for instantaneous behaviour

Instantaneous behaviour				
Mixes	N-SCC-a	N-SCC-b	D-SCC-a	D-SCC-b
Experimental Results	99.000	100.000	96.000	99.000
Eurocode 2 (1991)	94.634	94.634	94.634	94.634
CEB-FIP (1990)	82.656	82.656	82.656	82.656
ACI318-99 (1999)	161.199	161.199	161.199	161.199
Eurocode 2 (2004)	160.878	160.878	160.878	160.878
fib-Model Code (2010)	82.656	82.656	82.656	82.656
Nejadi (2005)	155.614	156.614	131.272	131.272
Leutbecher (2007)	82.656	82.656	82.656	82.656
Proposed Model	111.585	112.585	111.721	111.721
Mixes	S-SCC-a	S-SCC-b	DS-SCC-a	DS-SCC-b
Experimental Results	96.000	93.000	102.000	94.000
Eurocode 2 (1991)	94.634	94.634	94.634	94.634
CEB-FIP (1990)	82.656	82.656	82.656	82.656
ACI318-99 (1999)	161.199	161.199	161.199	161.199
Eurocode 2 (2004)	160.878	160.878	160.878	160.878
fib-Model Code (2010)	82.656	82.656	82.656	82.656
Nejadi (2005)	131.272	131.272	131.394	131.394
Leutbecher (2007)	82.656	82.656	82.656	82.656
Proposed Model	111.721	111.721	111.843	111.843

Table 4 Comparison between crack widths experimental results, proposed analytical model and codes for time-dependent behaviour

Time-dependent behaviour				
Mixes	N-SCC-a	N-SCC-b	D-SCC-a	D-SCC-b
Experimental results	0.2400	0.1800	0.2200	0.1400
Eurocode 2 (1991)	0.1551	0.1042	0.1551	0.1042
CEB-FIP (1990)	0.2030	0.1681	0.1905	0.1444
ACI318-99 (1999)	0.1785	0.1311	0.1783	0.1310
Eurocode 2 (2004)	0.1209	0.0757	0.1201	0.0627
fib-model code (2010)	0.1340	0.1108	0.1254	0.0943
Nejadi (2005)	0.1551	0.1061	0.1412	0.0944
Leutbecher (2007)	0.1962	0.1613	0.1823	0.1474
Proposed model	0.2224	0.1806	0.2026	0.1431
Mixes	S-SCC-a	S-SCC-b	DS-SCC-a	DS-SCC-b
Experimental results	0.2200	0.1500	0.2000	0.1400
Eurocode 2 (1991)	0.1551	0.1042	0.1551	0.1043
CEB-FIP (1990)	0.1978	0.1676	0.1999	0.1703
ACI318-99 (1999)	0.1783	0.1310	0.1782	0.1309
Eurocode 2 (2004)	0.1215	0.0763	0.1142	0.0690
fib-model code (2010)	0.1306	0.1106	0.1318	0.1123
Nejadi (2005)	0.1576	0.1083	0.1525	0.1039
Leutbecher (2007)	0.1975	0.1626	0.1942	0.1592
Proposed model	0.2270	0.1551	0.2089	0.1570

Table 5 Comparison between crack spacing experimental results, proposed analytical model and codes for instantaneous behaviour

Time-dependent Behaviour				
Mixes	N-SCC-a	N-SCC-b	D-SCC-a	D-SCC-b
Experimental Results	97.000	95.000	95.000	95.000
Eurocode 2 (1991)	94.634	94.634	94.634	94.634
CEB-FIP (1990)	82.656	82.656	82.656	82.656
ACI318-99 (1999)	161.199	161.199	161.199	161.199
Eurocode 2 (2004)	160.878	160.878	160.878	160.878
fib-Model Code (2010)	82.656	82.656	82.656	82.656
Nejadi (2005)	109.904	109.904	92.600	92.600
Leutbecher (2007)	82.656	82.656	82.756	82.756
Proposed Model	102.077	102.077	100.077	100.077
Mixes	S-SCC-a	S-SCC-b	DS-SCC-a	DS-SCC-b
Experimental Results	94.000	91.000	98.000	90.000
Eurocode 2 (1991)	94.634	94.634	94.634	94.634
CEB-FIP (1990)	82.656	82.656	82.656	82.656
ACI318-99 (1999)	161.199	161.199	161.199	161.199
Eurocode 2 (2004)	160.878	160.878	160.878	160.878
fib-Model Code (2010)	82.656	82.656	82.656	82.656
Nejadi (2005)	92.600	92.600	92.584	92.584
Leutbecher (2007)	82.756	82.756	82.847	82.847
Proposed Model	100.077	100.077	100.062	100.062

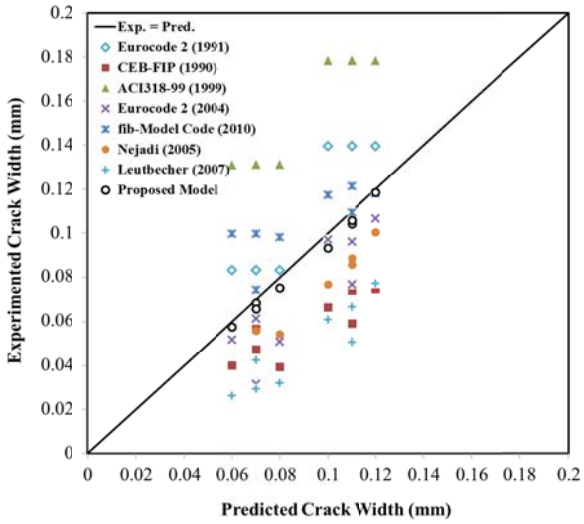

Fig. 10 Comparison between crack widths experimental results, proposed analytical model and codes for instantaneous behaviour

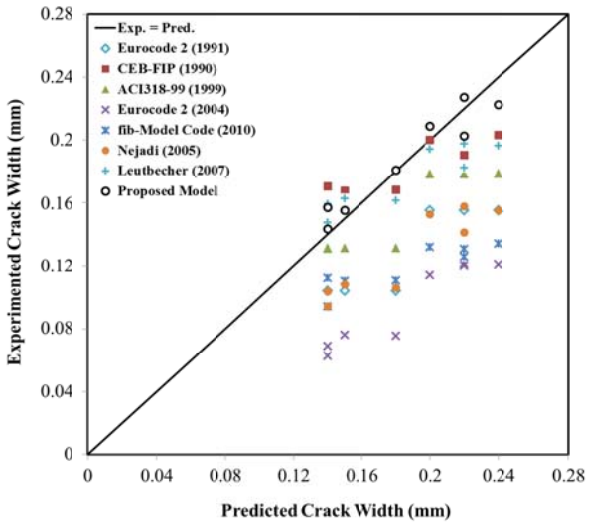

Fig. 11 Comparison between crack widths experimental results, proposed analytical model and codes for time-dependent behaviour

models corresponds to the quasi-permanent loading and underestimates the instantaneous crack spacing, but provides reasonable agreement with the measured final long-term crack spacing.

The crack spacing calculated in accordance with ACI318-99 (1999) and Eurocode 2 (2004) overestimate the short-term and long-term crack spacing. Due to the random nature of cracking, great accuracy in calculating the crack spacing is not achievable. Nevertheless, the instantaneous and final average crack spacing predicted by the Proposed Model is in good agreement with the measured instantaneous and final average crack spacing.

8. Conclusions

The following conclusions can be drawn from this study

- The Eurocode 2 (1991), ACI318-99 (1999), and fib-Model Code (2010) instantaneous crack width models are conservative.
- The Leutbecher (2007) and CEB-FIP (1990) time-dependent crack width models are conservative.
- The crack widths calculated in accordance with proposed model at steel stress levels up to 250 MPa shows that proposed model predicts crack widths which are in good agreement with the measured experimental results at all steel stress levels.
- The ACI318-99 (1999) and Eurocode 2 (2004) short-term and long-term crack spacing models are conservative.
- Due to the random nature of cracking, great accuracy in calculating the crack spacing is not achievable. Nevertheless, the instantaneous and final average crack spacing predicted by the proposed model in this study proves good agreement with the measured instantaneous and final average crack spacing.

References

ACI318-99 (1999), "Building code requirements for structural concrete", ACI 318-99, Detroit, American Concrete Institute.

AS 3600 (2009), "Concrete structures", Australian Standards.

Aslani, F. (2013), "Effects of specimen size and shape on compressive and tensile strengths of self-compacting concrete with or without fibers", *Mag. Concrete. Res.*, **65**(15), 914-929.

Aslani, F. (2014), "Experimental and numerical study of time-dependent behaviour of reinforced self-compacting concrete slabs", Ph.D Thesis, University of Technology, Sydney.

Aslani, F. (2015), "Creep behaviour of normal-and high-strength self-compacting concrete", *Struct. Eng. Mech.*, **53**(5), 921-938.

Aslani, F. and Nejadi, S. (2012a), "Mechanical properties of conventional and self-compacting concrete: an analytical study", *Constr. Build. Mater.*, **36**, 330-347.

Aslani, F. and Nejadi, S. (2012b), "Bond characteristics of steel fibre reinforced self-compacting concrete", *Can. J. Civil. Eng.*, **39**(7), 834-848.

Aslani, F. and Nejadi, S. (2012c), "Bond behavior of reinforcement in conventional and self-compacting concrete", *Adv. Struct. Eng.*, **15**(12), 2033-2051.

Aslani, F. and Nejadi, S. (2012d), "Shrinkage behavior of self-compacting concrete", *J. Zhejiang. Univ. Sci. A.*, **13**(6), 407-419.

Aslani, F. and Nejadi, S. (2012e), "Bond characteristics of reinforcing steel bars embedded in self-compacting concrete", *Aust. J. Struct. Eng.*, **13**(3), 279-295.

Aslani, F. and Nejadi, S. (2013a), "Self-compacting concrete incorporating steel and polypropylene fibers: compressive and tensile strengths, moduli of elasticity and rupture, compressive stress-strain curve and energy dissipated under compression", *Compos. Part. B – Eng.*, **53**, 121-133.

Aslani, F. and Nejadi, S. (2013b), "Creep and shrinkage of self-compacting concrete with and without fibers", *J. Adv. Concr. Technol.*, **11**(10), 251-265.

Aslani, F., Nejadi, S. and Samali, B. (2014a), "Short term bond shear stress and cracking control of reinforced self-compacting concrete one way slabs under flexural loading", *Comput. Concrete.*, **13**(6), 709-737.

Aslani, F., Nejadi, S. and Samali, B. (2014b), "Long-term flexural cracking control of reinforced self-compacting concrete one way slabs with and without fibres", *Comput. Concrete.*, **14**(4), 419-443.
Bishoff, P.H. (2003), "Tension stiffening and cracking of steel fiber reinforced concrete", *J. Mater. Civil. Eng.*, **15**(2), 174-182.
Broms, B.B. and Lutz, L.A. (1965), "Effects of arrangement of reinforcement on crack width and spacing of reinforced concrete members", *ACI. J. Proc.*, **62**(11), 1395-1410.
CEB-FIP. (1990), "High-strength Concrete State of the Art Report", Thomas Telford, London.
Chiaia, B., Fantilli, A.P. and Vallini, P. (2008), "Crack patterns in reinforced and fiber reinforced concrete structures", *Open. Constr. Build. Technol. J.*, **2**,146-155.
Eurocode 2. British Standards Institution, (1991), "Design of concrete structures-Part 1: General rules and rules for buildings", DD ENV 1991-1-1:1991. European Committee for Standardization, Brussels.
Eurocode 2. British Standards Institution, (2004), "Design of concrete structures-Part 1-1: General rules and rules for buildings", BS EN 1992-1-1:2004. European Committee for Standardization, Brussels.
Fib model code. (2010), "First complete draft Volume 1, fib Bulletin 55".
Gergely, P. and Lutz, L.A. (1968), "Maximum crack width in reinforced concrete flexural members", Causes, Mechanism, and Control of Cracking in Concrete , SP-20, American Concrete Institute, Detroit, 87-117.
Gilbert, R.I. and Nejadi, S. (2004), "An experimental study of flexural cracking in reinforced concrete members under sustained loads", UNICIV Report No. R-435, School of Civil and Environmental Engineering, University of New South Wales, Sydney, Australia.
Gilbert, R.I. and Ranzi, G. (2011), "Time-dependent Behaviour of Concrete Structures", Spon Press, New York.
Gribniak, V., Kaklauskas, G., Kliukas, R. and Jakubovskis, R. (2013), "Shrinkage effect on short-term deformation behavior of reinforced concrete-when it should not be neglected", *Mater. Design.*, **51**, 1060-1070.
Leutbecher, T. (2007), "Rissbildung und Zugtragverhalten von mit Stabstahl und Fasern bewehrtem Ultrahochfesten Beton (UHPC)", Doktors der Ingebieurwissenschaften genehmigte Dissertation, der Universitat Kassel.
Leutbecher, T. and Fehling, E. (2008), "Crack Formation and Tensile Behaviour of UHPC Reinforced with a Combination of Rebars and Fibres", (Eds., Schmidt, M., Fehling, E., Stürwald, S.) Ultra High Performance Concrete (UHPC), *Proceedings of the Second International Symposium on Ultra High Performance Concrete Structural Materials and Engineering Series*, **10**, 497-504.
Marí, A.R. Bairán, J.M. and Duarte, N. (2010), "Long-term deflections in cracked reinforced concrete flexural members", *Eng. Struct.*, **32**(3), 829-842
Marti, P., Alvarez, M., Kaufmann, W. and Sigrist, V. (1998), "Tension chord model for structural concrete", *Struct. Eng. Int.*, **8**(4), 287-298.
Mazzotti, C. and Savoia, M. (2009), "Long-term deflection of reinforced self-consolidating concrete beams", *ACI . Struct. J.*, **6**(6), 772-781.
Nejadi, S. (2005), "Time-dependent cracking and crack control in reinforced concrete structures", Ph.D Thesis, The University of New South Wales.
RILEM TC 162-TDF. (2002), "Test and design methods for steel fibre reinforced concrete", Final recommendations, *Mater. Struct.*, **35**, 579-582.
Vasanelli, E., Micelli, F., Aiello, M.A. and Plizzari, G. (2013), "Long term behavior of FRC flexural beams under sustained load", *Eng. Struct.*, **56**, 1858-1867.